Synthetic Lipid Vesicles Recruit Native-Like Aggregates and Affect the Aggregation Process of the Prion Ure2p: Insights on Vesicle Permeabilization and Charge Selectivity

Laura Pieri,[†‡] Monica Bucciantini,[†‡*] Patrizio Guasti,[§] Jimmy Savistchenko,[¶] Ronald Melki,[¶*] and Massimo Stefani[†]

[†]Department of Biochemical Sciences, [‡]Research Centre on the Molecular Basis of Neurodegeneration, and [§]Department of Anatomy, Histology, and Forensic Medicine, University of Florence, Italy; and [¶]Laboratoire d'Enzymologie et Biochimie Structurales, Centre National de la Recherche Scientifique, 91198 Gif-Sur-Yvette cedex, France

ABSTRACT The yeast prion Ure2p polymerizes into native-like fibrils, retaining the overall structure and binding properties of the soluble protein. Recently we have shown that, similar to amyloid oligomers, the native-like Ure2p fibrils and their precursor oligomers are highly toxic to cultured mammalian cells when added to the culture medium, whereas Ure2p amyloid fibrils generated by heating the native-like fibrils are substantially harmless. We show here that, contrary to the nontoxic amyloid fibrils, the toxic, native-like Ure2p assemblies induce a significant calcein release from negatively charged phosphatidylserine vesicles. A minor and less-specific effect was observed with zwitterionic phosphatidylcholine vesicles, suggesting that the toxic aggregates preferentially bind to negatively charged sites on lipid membranes. We also found that cholesterol-enriched phospholipid membranes are protected against permeabilization by native-like Ure2p assemblies. Moreover, vesicle permeabilization appears charge-selective, allowing calcium, but not chloride, influx to be monitored. Finally, we found that the interaction with phosphatidylserine membranes speeds up Ure2p polymerization into oligomers and fibrils structurally and morphologically similar to the native-like Ure2p assemblies arising in free solution, although less cytotoxic. These data suggest that soluble Ure2p oligomers and native-like fibrils, but not amyloid fibrils, interact intimately with negatively charged lipid membranes, where they allow selective cation influx.

INTRODUCTION

Transmissible spongiform encephalopathies, including human Creutzfeldt-Jacob disease, bovine spongiform encephalopathy, and sheep scrapie, are neurodegenerative diseases arising from the polymerization into fibrillar amyloid assemblies of the prion protein (PrP^{c}) structurally altered in an amyloidogenic conformation (PrP^{sc}) (1). Prion proteins have also been described in yeasts and fungi. For example, the yeast *Saccharomyces cerevisiae* exhibits three prion traits. The [*URE3*] trait, which is heritable in a non-Mendelian manner, arises from the protein Ure2 and results in a modified regulation of nitrogen catabolism (2–4).

Native Ure2p is a dimeric cytosolic protein that becomes inactive and insoluble in the cytoplasm of the [*URE3*] yeast cells, where it forms large globular or elongated aggregates (5). Ure2p is a two-domain protein containing a flexible and poorly structured N-terminal ''prion'' domain (residues 1–93) required for in vitro fibril formation and prion propagation (6,7) and a folded globular, α-helical C-terminal domain (residues 95–354) (7–9) whose crystal structure has been determined (10,11). The C-terminal domain shares sequence and fold homologies with proteins of the glutathione *S*-transferase family (12,13). Actually, in its native, soluble state, Ure2p binds glutathione (14) and displays a multisubstrate glutathione peroxidase activity (15).

Under physiological conditions, recombinant Ure2p assembles in vitro into globular oligomers eventually giving rise to fibrils displaying several morphological, structural, and tinctorial features of amyloids, including enhanced resistance to proteolysis, increased Thioflavin T (ThT) fluorescence, and the yellow-green birefringence in cross-polarized light upon Congo red binding (8,16). However, these fibrils possess several characteristics that set them apart from conventional amyloid fibrils. In fact, they lack the cross-β framework typical of amyloids (17), and the Ure2p monomers assembled in these fibrils retain their native structure, the ability to bind glutathione, and the glutathione peroxidase activity (18,15). Thus, Ure2p aggregation into native-like fibrils is reminiscent of the assembly of specific proteins into functional polymers, such as actin filaments and microtubules, or into pathological polymers such as serpin polymers (19). These results have led to propose a model of Ure2p assembly into native-like fibrils based on the assumption that only minor conformational changes occur during the process (18,20).

Native-like Ure2p fibrils incubated at 60°C for 1 h undergo major conformational changes involving the organization of a cross-β core typical of amyloid fibrils, as revealed by the x-ray diffraction images, with the appearance of the characteristic reflection at 4.7 Å that is missing in the diffraction pattern of native-like fibrils (21). Such a change in

Submitted October 10, 2008, and accepted for publication December 23, 2008.

*Correspondence: monica.bucciantini@unifi.it or melki@lebs.cnrs-gif.fr

Editor: Ruth Nussinov.

0006-3495/09/04/3319/12 $2.00

doi: 10.1016/j.bpj.2008.12.3958

native-like fibrils is accompanied by the loss of their ability to bind glutathione, by a significant increase of their β-sheet content, and by a significant change in their proteolytic pattern, probably arising from increased packing of Ure2p molecules within the fibrils. Despite their structural differences, the heat-treated Ure2p fibrils are undistinguishable from the native-like fibrils on negatively stained electron micrographs (21).

In a recent study, we have shown that Ure2p native-like assemblies (dimers, oligomers, and fibrils) are highly toxic to cultured mammalian cells when added to the culture medium, whereas the amyloid fibrils obtained by heat treatment of the toxic native-like fibrils appear harmless (22). Similar to Ure2p, p13suc1, a small protein that can exist as a monomer and as a domain-swapped dimer, assembles into cytotoxic native-like aggregates (23). These results led to hypothesize that the toxicity of protein aggregates cannot be considered as a specific property of amyloid assemblies; rather it can also be displayed by protein assemblies where the polypeptide units maintain their overall native structure.

Based on our previous observations, we proposed that the toxicity of Ure2p native-like aggregates depends on their ability to interact with the cell surface, similarly to amyloids, resulting in membrane permeabilization, deregulation of free Ca^{2+} homeostasis, oxidative stress, and eventually cell death (22). This view is consistent with the widely accepted idea that the toxicity of protein aggregates is mainly the consequence of their interaction with the cell membranes; such an interaction is reminiscent of the behavior of pore-forming proteins such as bacterial toxins (24,25), with alteration of membrane permeability and imbalance of ion homeostasis (26,27).

An increasing body of evidence indicates that surfaces, notably synthetic and biological membranes, are able to speed up protein/peptide aggregation behaving as conformational catalysts in a two-dimensional environment (28). In particular, surfaces can accelerate aggregate nucleation by recruiting the monomers with significant increase of their local concentration and favoring monomer unfolding (29). The structural features of amyloid fibrils grown on surfaces can depend on the type of surface and can be different from those displayed by fibrils arising in solution. These effects are associated with the physicochemical properties of the surface, and in particular, in the case of lipid surfaces, with the lipid composition that, in turn, affects the physical properties of the membrane including charge, hydrophobicity, fluidity, density of packing, curvature, and others (30).

Under physiological conditions protein/peptide aggregation occurs in an intracellular or extracellular crowded environment. Thus, describing the mechanism of protein/peptide aggregation in tissues and the influence of cell membranes is of the utmost importance as it may allow understanding the molecular events leading to this aggregation and the associated cytotoxicity (31,32). Here we documented the interaction between different native-like Ure2p assemblies and synthetic phospholipid unilamellar vesicles to provide additional information on the molecular features that induce plasma membrane permeabilization, a key event underlying amyloid and nonamyloid aggregate cytotoxicity. We also investigated the ability of lipid membranes to act as catalysts of Ure2p aggregation into fibrillar assemblies, possibly by inducing conformational changes that could influence the aggregation pathway and eventually the nature and/or the toxicity of the resulting Ure2p assemblies.

The interaction of native-like and amyloid Ure2p aggregates with synthetic phosphatidylcholine (PC); phosphatidylserine (PS); PC/PS mixed vesicles; and, in some cases, PS vesicles enriched in cholesterol was documented. The leakage through the vesicle membrane of differently sized chemicals (calcein) or charged ions (Ca^{2+}, Cl^{-}) was also investigated. We found that the toxic, native-like Ure2p assemblies interact preferentially with negatively charged membranes, inducing significant calcein release from PS or PS-enriched vesicles, whereas no significant permeabilization was induced by the nontoxic heat-treated amyloid fibrils. Furthermore, cholesterol enrichment protects membranes against permeabilization by the Ure2p assemblies. We also found that vesicle permeabilization by the Ure2p native-like oligomers and fibrils is at least charge selective, allowing movements of positively charged ions such as Ca^{2+}, but not of anions such as Cl^{-}.

MATERIALS AND METHODS

Ure2p assembly into oligomers and fibrils

Ure2p was expressed in *Escherichia coli*, purified as previously described (7,8), and stored at −80°C in buffer A (20 mM Tris-HCl, pH 7.5, 200 mM KCl, 1 mM dithiothreitol, 1 mM EGTA). Ure2p assembly into native-like fibrils was achieved by incubating the protein (50–100 μM) at 8°C without shaking in buffer A for 48–96 h. Soluble Ure2p oligomers were obtained soon after thawing the protein stored at −80°C. Ure2p amyloid fibrils were obtained by heating the native-like fibrils at 60°C for 1 h .

Preparation of phospholipid unilamellar vesicles

Lipids were purchased from Avanti Polar Lipids (Alabaster, AL). 1,2-Dioleoyl-*sn*-glycero-3-[phospho-L-serine], 1,2-dioleoyl-*sn*-glycero-3-phosphocholine, 1,2-dioleoyl-*sn*-glycero-3-[phospho-*rac*-(1-glycerol)], and cholesterol in chloroform solutions were dried in glass tubes (8 mm in diameter) under a gentle nitrogen stream in a fume hood. For mixed lipid membrane and lipid/cholesterol preparations, chloroform solutions were mixed in the appropriate ratio before evaporation. For calcein release assay, the dry lipid film resulting from evaporation was resuspended in 60 mM calcein (Sigma, St. Louis, MO), 1 M Tris-HCl buffer, pH 7.5, at a 1 mg/ml final lipid concentration. For Ca^{2+} influx measurements, the lipid film was resuspended in 0.1 mM Fura-2 (Molecular Probes, Eugene, OR), 20 mM Tris-HCl buffer, pH 7.5, 200 mM KCl, at a final lipid concentration of 20 mg/ml. For Cl^{-} influx measurements, the lipid film was resuspended in 1 mM lucigenin (Molecular Probes), in 200 mM KNO_3 solution at a final lipid concentration of 10 mg/ml. For circular dichroism (CD) analysis, ThT assay, cytotoxicity assay, and EM analysis, the lipid film was resuspended in buffer A. The resuspended samples were incubated for 1 h at room temperature to allow lipid hydration and vesicle formation, vortexing occasionally. After

1 h, the lipid suspensions were vigorously vortexed to allow complete detachment of hydrated lipids. The resulting suspension was subjected to five freeze-thaw cycles of 2 min each: freezing in liquid nitrogen followed by 2 min thawing at 37°C. Then the sample was sonicated for 20 min at 20 kHz in ice to obtain a clear suspension of small unilamellar vesicles. The large lipid aggregates and titanium impurities coming from the sonicator probe were removed by centrifuging the preparation for 10 min at 10,000 × g. For permeabilization experiments using vesicles loaded with fluorescent compounds, the nonencapsulated fluorescent markers were removed by gel-filtration using a Sephadex G-50 column (1.5 × 7.5 cm); the eluted vesicles were used within 48 h. Before each experiment, the size distribution of the vesicle population was checked using a Zetasizer Nano S dynamic light scattering device from Malvern Instruments (Malvern, Worcestershire, UK). Nonhomogeneous lipid populations, i.e., preparations where the mean size was not comprised in the range 50–100 nm, were discarded.

Calcein release assay

Calcein-loaded lipid PS or PC vesicles were incubated in buffer A in the presence of the different types of Ure2p aggregates at 25°C and 15°C, respectively. These temperatures take into account the different phase transition temperature (Tm) of PS and PC (−11°C and −20°C, respectively).

The calcein is self-quenched in the vesicle acqueous core; therefore, calcein leakage to the external medium upon Ure2p aggregate-vesicle interaction can be monitored as increase of calcein fluorescence due to calcein dilution and consequent reduction of self-quenching. The measurements were performed in real-time using a 2 × 10-mm path length cuvette and a PerkinElmer (Waltham, MA) LS55 spectrofluorimeter equipped with a thermostated cell holder. The excitation and emission wavelengths were 490 nm and 520 nm, respectively; the excitation and emission slits were set at 15 nm and 2,5 nm, respectively. The percentage of calcein release was calculated according to the ratio

$$\%\ \max\ =\ (F - F_0)\ \times\ 100/(F_{\max} - F_0),$$

where F is the fluorescence measured at the different time intervals during the experiment, F_0 is the fluorescence measured at the beginning of the experiment, and $F_{\max}$ is the maximum fluorescence, as determined by disrupting the vesicles at the end of each experiment by adding 0,1% Triton X-100.

Measurement of Ca^{2+} influx

Fura-2-loaded PS or PC vesicles were incubated in 20 mM Tris-HCl buffer, pH 7.5, 200 mM KCl, 1 mM DTT in the presence of the different types of Ure2p aggregates, as described above. To establish a Ca^{2+} gradient across the lipid membrane, 1 mM $CaCl_2$ was added to the solution at the beginning of each measurement. Such a Ca^{2+} concentration was chosen to ensure conditions under which the Ca^{2+} is in excess respect to the Fura-2 probe without inducing vesicle aggregation or fusion.

The Ure2p aggregate-induced Ca^{2+} influx into the vesicles was monitored by following the changes over time of the fluorescence ratio of the Ca^{2+}-sensitive fluorophore Fura-2 at excitation wavelengths of 340 nm and 380 nm (F340/F380) due to the Ca^{2+} binding by Fura-2 (33) with an emission wavelength of 515 nm. Fura-2 exhibits a shift in the excitation wavelength from 380 nm to 340 nm upon Ca^{2+} binding. The excitation and emission slits were both set at 5 nm. The Ca^{2+} influx was reported as percentage of the maximum fluorescence ratio F340/F380 corresponding to full complexation of Fura-2 by Ca^{2+} obtained after addition of 100 nM ionomycin (Molecular Probes), a ionophore that allows Ca^{2+} passive diffusion through the lipid bilayer, according to the ratio:

$$\%\ \max\ =\ (R - R_0)\ \times\ 100/(R_{\max} - R_0),$$

where R is the fluorescence ratio F340/F380 measured at the different time intervals during the experiment, R_0 is the fluorescence ratio measured at the beginning of the experiment, and $R_{\max}$ is the maximum fluorescence ratio, corresponding to the maximum Ca^{2+} influx, determined by adding 100 nM ionomycin at the end of each experiment.

The effect of tromethamine (10 mM), a potent inhibitor of ion mobility through channels made of amyloid forming peptides, on Ca^{2+} influx was documented as described (34).

Measurement of Cl^- influx

To monitor Cl^- influx into vesicles incubated in the presence of native-like Ure2p aggregates, we used the fluorescent Cl^--sensitive probe lucigenin (bis-*N*-methylacridinium nitrate). This probe is known to be collisionally quenched by halide ions resulting in a decrease of the ion concentration-dependent fluorescence without any shift in wavelength; this method has been used to detect Cl^- transport by biological carriers (35). Briefly, lucigenin-loaded PS and PC vesicles were incubated in 20 mM Tris-HCl buffer, pH 7.5, containing 200 mM KNO_3, 1 mM EGTA, and 1 mM DTT in the presence of the different types of Ure2p aggregates, as described above. To establish a Cl^- gradient across the lipid membrane, 20 mM KCl was added to the solution at the beginning of each measurement. To maintain the osmolarity of buffer A, KCl was replaced by 200 mM KNO_3 because nitrate is lipophilic with respect to other anions and therefore can cross easily the lipid bilayer. It therefore appears able to counteract the electrostatic potential created by the possible influx of Cl^- ions into the vesicles, thus enhancing such an influx (35).

The Cl^- influx over time was monitored by measuring the changes in the fluorescence of lucigenin, collisionally quenched by Cl^-; therefore, the influx of Cl^- into the vesicles was measured as a decrease of the initial fluorescence. The minimum fluorescence value, corresponding to complete quenching of lucigenin fluorescence by Cl^-, was obtained by adding, at the end of each measurement, 10 μM of the Cl^- ionophore tributyltin (Sigma), an organometallic compound that acts as a Cl^-/OH^- antiporter (36). This value was used to normalize the data. The normalization was obtained according to the following calculation:

$$\%\ =\ 100 - [(F - F_{\min})\ \times\ 100/(F_0 - F_{\min})],$$

where F is the lucigenin fluorescence measured at different time intervals during the experiment; $F_{\min}$ is the minimum fluorescence, corresponding to the maximum Cl^- influx, determined by adding 10 μM tributyltin at the end of each experiment; and F_0 is the maximum fluorescence measured at the beginning of the experiment. The measurements were performed in real-time using a 2 × 10-mm path length cuvette and a PerkinElmer LS55 spectrofluorimeter equipped with a thermostated cell holder. The excitation and emission wavelengths were set at 455 nm and 505 nm, respectively, and the excitation and emission slits were both set at 5 nm.

Electron microscopy

Electron micrographs were acquired using a JEM 1010 transmission electron microscope at 80 kV excitation voltage. To investigate the interaction between lipid vesicles and preformed Ure2p aggregates, PS or PC small unilamellar vesicles were diluted in buffer A at a final concentration of ~600 μM in the presence or absence of 10 μM of the different types of Ure2p assemblies and incubated at 25°C for 15 min. Based on the permeabilization data, these conditions are suitable to observe a significant interaction between Ure2p and membranes. To investigate the mutual interaction between lipid vesicles and Ure2p during protein assembly, Ure2p was incubated for 1 h or 48 h at a concentration of 50 μM in the absence or in the presence of 1.2 mM PS or PC vesicles at 4°C without shaking. After the incubation, the lipid suspensions were adsorbed onto formvar/carbon-coated 400 mesh nickel grids (Agar Scientific, Stansted, UK) by floating the grids onto 10 μl drops of the lipid-protein sample. Then the grids were blotted and, after drying, negatively stained with 2% (w/v) uranyl acetate (Sigma). After

wicking off the excess stain, the grids were allowed to air-dry and observed under the electron microscope.

ThT binding assay

The effect of PS and PC vesicles on Ure2p assembly was investigated by ThT binding assay (37). For these experiments, Ure2p was incubated at a concentration of 50 μM in the absence or presence of 1.2 mM PS or PC vesicles at 4°C without shaking. Sample aliquots of 10 μl were mixed at regular time intervals with 400 μl of 10 μM ThT. The resulting fluorescence was measured at excitation and emission wavelengths of 440 nm and 480 nm, respectively, as previously described (38).

CD measurements

For CD measurements, Ure2p was diluted in buffer A at a final concentration of 25 μM in the presence or in the absence of 600 μM PS. Far-UV CD spectra of Ure2p with or without PS vesicles were acquired at 25°C using a 1-mm path length quartz cuvette and a Jasco J-810 spectropolarimeter (Great Dunmow, Essex, UK) equipped with a thermostated cell holder. Each spectrum was obtained by calculating the average of four scans and subtracting the appropriate blank. For each sample, the first set of spectra was acquired immediately after Ure2p addition to the PS solution. Other spectra were acquired over time during Ure2p incubation in the presence of vesicles for 48 h.

The spectra were recorded in the 260–190 nm range at a speed of 50 nm/min. The mean residue molar ellipticity [Θ] in millidegrees was calculated using the formula

$$[\Theta] = \Theta/10\, n\, Cl,$$

where n is the number of residues, C is the molar concentration of the protein, and l is the path length in centimeters.

Cell culture and cell viability assay

Murine endothelioma H-END cells were used as a cell model to investigate Ure2p assembly cytotoxicity. The cells were provided by Prof. F. Bussolino (University of Turin, Italy) and cultured in Dulbecco's modified Eagle's medium containing 10% fetal bovine serum, 3 mM glutamine, 100 units/ml penicillin, and 100 μg/ml streptomycin. All materials used for cell culture were from Sigma. The toxicity of Ure2p aggregates formed in the presence or in the absence of PS vesicles was assessed by the 3-(4,5-dimethylthiazol-2-yl)-2,5-diphenyltetrazolium bromide (MTT) reduction inhibition test (39).

H-END cells were plated at a density of 1500 cells per well on 96-well plates in 100 μl of culture medium. After 48 h, the medium was exchanged with 100 μl of fresh medium containing 10 μM of the different Ure2p aggregates. Then the cells were incubated for 24 h in the presence of the aggregates. Controls were performed by supplementing the cell cultures with identical volumes of buffer A with or without PS vesicles for the same length of time. After incubation, the cells were treated for another 2 h with 100 μl of serum-free Dulbecco's modified Eagle's medium without phenol red, containing 0.5 mg/ml MTT. Then 100 μl of cell lysis solution (20% SDS, 50% *N*,*N*-dimethylformamide) was added to each well, and the samples were incubated at 37°C to allow complete lysis. The absorbance values of blue formazan were determined at 570 nm with an automatic plate reader (Bio-Rad, Hercules, CA).

RESULTS

Calcein release from lipid vesicles induced by Ure2p aggregates

Membrane disassembly and permeabilization are well-known effects of prefibrillar amyloid assemblies. Less information is available on the possible effects on biological or synthetic lipid membranes of oligomers and fibrils where the constituent protein monomers retain a substantially native fold. To provide data on this topic, we investigated lipid membrane perturbation by native-like Ure2p aggregates and the amyloid fibrils arising from heat-treatment of the Ure2p native-like fibrils. To this purpose, we measured the extent of calcein release from unilamellar vesicles of different lipid composition after incubation with the different forms of Ure2p assemblies. Neutral, zwitterionic (PC), or negatively charged (PS and PG) phospholipid vesicles were used together with mixed PC/PS or cholesterol-enriched PS vesicles. The use of vesicles with different lipid composition allowed us to assess the role played by electrostatic and hydrophobic interactions in the contact between Ure2p toxic assemblies and lipid membranes, as well as the importance of membrane fluidity modulation by cholesterol.

In a first set of experiments, we monitored for a 3 h time period, the vesicle permeabilizing effect of the different types of Ure2p aggregates incubated at a final concentration of 10 μM (protein monomer concentration). The results obtained are shown in Fig. 1. We observed a significant extent of calcein release from PS vesicles treated with native-like soluble Ure2p oligomers or fibrils (reaching 30–35% of the maximum release after 180 min), whereas no significant permeabilization was induced by the heat-treated, amyloid fibrils previously shown to be nontoxic (22) (Fig. 1 *A*). This result is consistent with the idea that, at variance with the harmless heat-treated amyloid fibrils, the toxic native-like Ure2p assemblies interact electrostatically with the negatively charged phospholipids.

The same experiments carried out with zwitterionic PC vesicles showed an initially similar extent of calcein release upon exposure to either toxic, native-like oligomers and fibrils or to nontoxic amyloid fibrils of Ure2p (Fig. 1 *B*); however, the final extent of calcein leakage resulting from the interaction of the native-like oligomers and fibrils with PC vesicles was significantly lower than that observed for PS vesicles (<25% of the maximum after 180 min), although the phenomenon was comparable during the first 30 min of incubation. In addition, vesicles treated with a 10-fold lower concentration of Ure2p (1 μM) showed similar responses (not shown), indicating that a much lower protein/lipid molar is sufficient to induce vesicle permeabilization. The moderate PC vesicle permeabilization could result from membrane damage by a nonspecific interaction of toxic and nontoxic protein assemblies as well as from a reduced stability of the vesicles. The higher permeabilizing effect of native-like Ure2p oligomers and fibrils on PS vesicles agrees with the large body of data relative to amyloid assemblies indicating that aggregate-membrane interaction is favored, at least in most cases, by the presence of negatively charged lipids (40,41).

We also investigated early vesicle permeabilization by limiting the time window to the first 30 min of vesicle

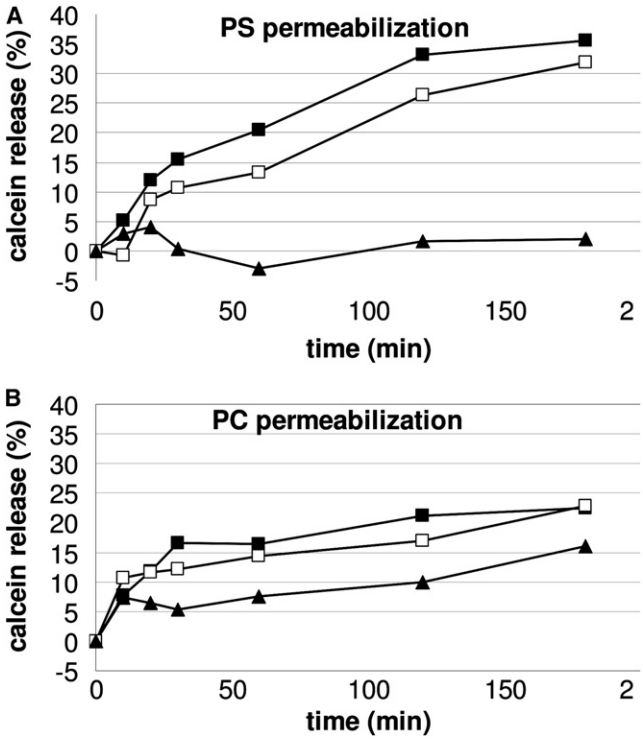

FIGURE 1 Calcein release induced in PS and PC vesicles by Ure2p aggregates. (*A*) Vesicles made of negatively charged PS; (*B*) vesicles made of zwitterionic PC. Protein aggregates were prepared as described under Materials and Methods and added to the calcein-loaded vesicle suspension at 10 μM final protein concentration; (□) native-like Ure2p fibrils, (■) soluble Ure2p oligomers, (▲) Ure2p amyloid fibrils. Control experiments were performed by diluting similarly the vesicles in buffer A without Ure2p, to take into account spontaneous membrane leakage. The points are reported as net values obtained by subtracting the percentage of spontaneous calcein release measured at each time in control vesicles from the release measured in vesicles treated with the different Ure2p aggregates. The values shown in each graph were obtained from one experiment out of at least three independent measurements yielding qualitatively identical results.

incubation with Ure2p aggregates. Fig. 2, *A–C*, shows the kinetics of calcein release from unilamellar PS, PC, and PG vesicles, respectively, incubated with the different types of Ure2p assemblies. The permeabilization kinetics confirm that the negatively charged PS vesicles display higher affinity for the native-like Ure2p assemblies than the neutral PC vesicles. To better assess the role played by the negatively charged PS in membrane disruption by soluble Ure2p oligomers and native-like fibrils, we also tested the permeabilization of PC vesicles containing 10% (w/w) PS. Interestingly, the moderate nonspecific PC vesicle permeabilization by the nontoxic, heat-treated Ure2p fibrils was lost in these PC/PS mixed vesicles, whereas the specificity for the toxic soluble oligomers and native-like fibrils was completely retained (Fig. 2 *D*). This suggests that moderate amounts of PS in zwitterionic membranes can be sufficient to create clusters of negative charges that could anchor Ure2p native-like assemblies to the membrane surface favoring subsequent membrane permeabilization. Moreover, the presence of PS increases PC vesicle stability thus avoiding the nonspecific leakage shown by PC vesicles exposed to heat-treated fibrils.

Cholesterol content plays a largely recognized role in modulating the ability of toxic amyloid aggregates to interact with, and to permeabilize, cell membranes. To evaluate the role, if any, of cholesterol in the interaction between Ure2p native-like assemblies and our synthetic lipid vesicles, we investigated the permeabilizing effect of Ure2p assemblies on unilamellar PS vesicles enriched in cholesterol (cholesterol/PS molar = 1:3). Interestingly, the incorporation of cholesterol resulted in a significant decrease of membrane permeabilization by Ure2p native-like assemblies. Actually, these vesicles displayed a remarkably decreased calcein release (<5%) (Fig. 2 *E*) when compared to PS vesicles (Fig. 2 *A*) treated with the same concentration of the same Ure2p aggregates. A similar loss of permeabilization was found in unilamellar vesicles prepared from brain lipid extracts treated with Ure2p assemblies (Fig. 2 *F*). Overall, these data suggest that a complex lipid composition can modulate the stability of the lipid bilayer, and thus its resistance to disruption by toxic protein aggregates. The data are also consistent with several experimental findings indicating that biological and synthetic lipid membranes enriched in cholesterol display increased resistance to permeabilization and disassembly by amyloid aggregates (42–44). Finally, our findings extend such behavior to aberrant protein assemblies where the monomers are maintained in native-like conformation.

Ure2p aggregates induce Ca^{2+} (but not Cl^-) influx into lipid vesicles

Many efforts have been made to characterize the molecular mechanisms of membrane permeabilization by toxic protein aggregates. An important step toward a better understanding of the features of membrane damage is assessing the size and/or charge selectivity of the discontinuites produced by aggregate interaction with the lipid bilayer. To test whether Ure2p toxic assemblies permeabilize lipid vesicles through the formation of charge-selective passages, we measured their selectivity with regard to the influx of positive and negative ions, namely Ca^{2+} and Cl^-. PS and PC unilamellar vesicles loaded with the fluorescent probes Fura-2 or lucigenin, respectively, were used for these measurements; the time-courses of Ca^{2+} or Cl^- influxes were monitored by measuring the fluorescence of Fura-2 or lucigenin entrapped inside the vesicles. Fig. 3, *A* and *B*, show the kinetics of Ca^{2+} influx into PS or PC unilamellar vesicles exposed for 25 min to the different Ure2p aggregates. A significant Ca^{2+} influx was observed for both types of vesicles. The extent of Ca^{2+} influx reached ~40–60% or ~20–25% of the maximum, upon vesicle incubation with native-like Ure2p fibrils or soluble oligomers, respectively. A minor membrane permeabilization (~10%) was induced by the heat-treated fibrils,

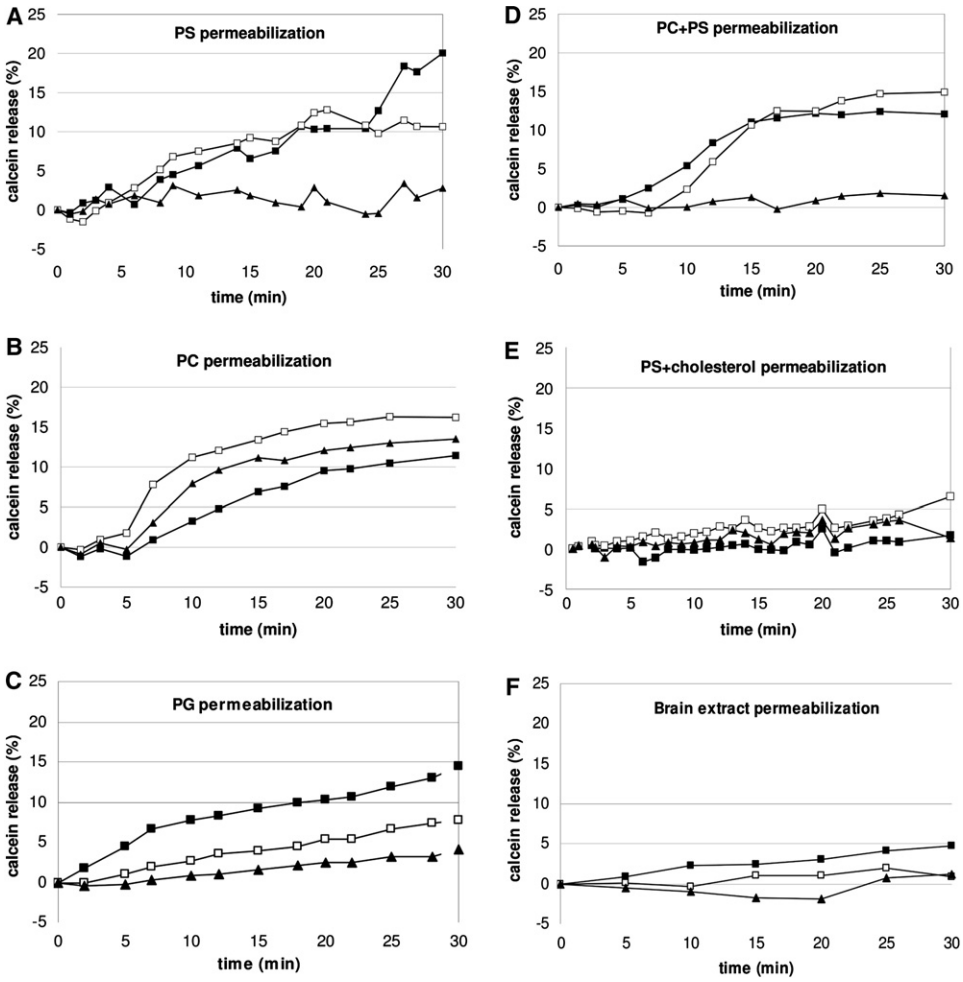

FIGURE 2 Calcein release induced in different types of unilamellar vesicles by Ure2p aggregates. (*A*) Vesicles made of negatively charged PS; (*B*) vesicles made of zwitterionic PC; (*C*) PG vesicles; (*D*) PC vesicles containing 10% negatively charged PS; (*E*) PS vesicles containing cholesterol (1:3 cholesterol/vesicle molar); (*F*) vesicles made of lipids extracted from brains. Protein aggregates were prepared as described under Materials and Methods and added to the calcein-loaded vesicle suspension at 1 μM (in *A*, *B*, *D*, *E*, and *F*) or 5 μM (in *C*) final protein concentration; (□) native-like Ure2p fibrils, (■) soluble Ure2p oligomers, (▲) Ure2p amyloid fibrils. Then the lipid-protein mixture was incubated directly in the cuvette, and the increase of fluorescence due to calcein release was monitored over time for 30 min. Control experiments were carried out by diluting the vesicles in the same way in buffer A without Ure2p, to take into account spontaneous membrane leakage. The points are reported as net values obtained after subtracting the percentage of spontaneous calcein release measured at each time in control vesicles from the release measured in vesicles treated with the different Ure2p aggregates. The values shown in each graph were obtained from one experiment out of at least three independent measurements yielding qualitatively identical results.

in agreement with the calcein leakage data reported above. We thus conclude that upon interacting with either PS or PC membranes, native-like Ure2p assemblies induce Ca^{2+} entry within the vesicles and that Ure2p native-like assemblies possess a significantly higher permeabilizing potential as compared to the amyloid form of the protein, in agreement with their higher toxicity level previously observed on cultured mammalian cells (22). Ca^{2+} permeabilization was concentration dependent (see the Supporting Material, Fig. S1) and linear in the 0–20 μM range. In addition, Ca^{2+} influx was abolished in the presence of 10 mM tromethamine, an inhibitor of ion mobility through channels made of amyloid forming polypeptides (see Fig. S2).

Interestingly, no significant Cl^- ions influxes could be detected in PS or PC vesicles treated with Ure2p aggregates (Fig. 3, *C* and *D*) even in the presence of nitrate ions, whose high lipophilicity enhances Cl^- influx by counteracting the electrostatic potential created by Cl^- translocation inside the vesicles (35). Vesicle permeabilization to Ca^{2+} ions, but not to Cl^- ions, suggests that ion entry into the vesicles cannot result from simple diffusion through lipid membrane discontinuities after destruction of membrane order by the native-like aggregates, but is directly mediated by the latter in a charge-selective fashion. Thus, Ure2p native-like assemblies appear to create within the membranes charge-selective passages that allow the entry of positively charged ions while hindering the influx of negatively charged ones.

Imaging of PS vesicle interaction with Ure2p native-like assemblies by electron microscopy

The physical relation between synthetic lipid vesicles and Ure2p aggregates was investigated by imaging the interaction of Ure2p toxic aggregates with lipid membranes by electron microscopy. Electron micrographs of negatively stained PS vesicle suspensions incubated for 15 min with native-like soluble Ure2p oligomers or fibrils are shown in Fig. 4, *A* and *B*. In these preparations, the Ure2p toxic assemblies were mainly localized in the vicinity of the vesicles, with small oligomers intimately associated with the vesicle surface (Fig. 4 *A*, *arrows*). Seemingly, the native-like fibrils interact with the vesicle surface through their ends or sides (Fig. 4 *B*). It is worth noting that the presence of Ure2p assemblies induces a fission process of the PS vesicles resembling a detergent-like effect (see below). Interestingly, the nontoxic heat-treated Ure2p amyloid fibrils were never observed to associate

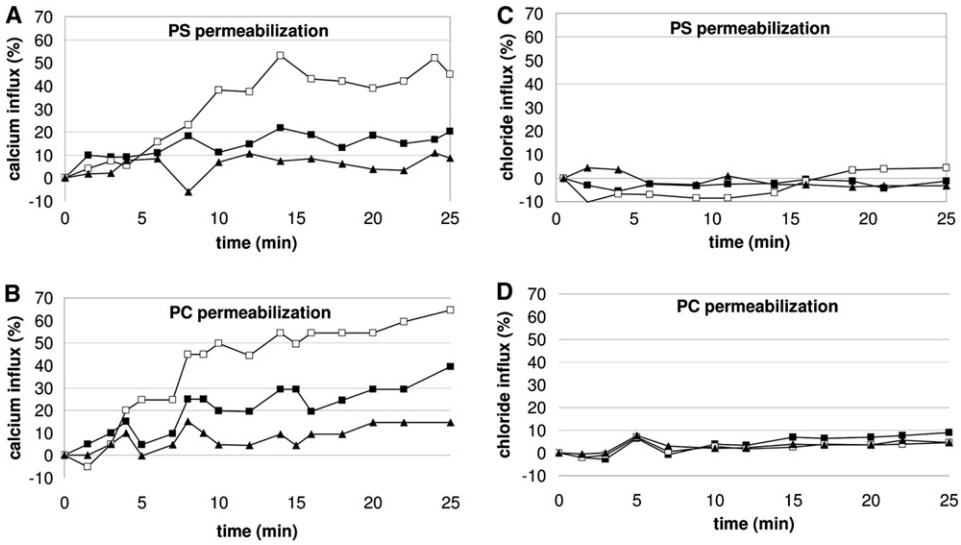

FIGURE 3 Ure2p aggregates allow Ca^{2+}, but not Cl^-, ion influxes into unilamellar vesicles. (*A* and *B*) Ca^{2+} influx (% max) into PS or PC vesicles, respectively. (*C* and *D*) Cl^- influx (% max) into PS or PC vesicles, respectively. For Ca^{2+} influx measurements, (□) native-like Ure2p fibrils, (■) soluble Ure2p oligomers, (▲) Ure2p amyloid fibrils were added to the suspension of vesicles loaded with 0.1 mM Fura-2 at 10 μM final protein concentration, in the presence of 1 mM $CaCl_2$. Then the lipid-protein mixture was incubated directly in the cuvette and the increase of Fura-2 fluorescence ratio F340/F380 due to Ca^{2+} influx into the vesicles was monitored over time for 25 min. For Cl^- influx measurements, (□) native-like Ure2p fibrils, (■) soluble Ure2p oligomers, (▲) Ure2p amyloid fibrils were added to the suspension of vesicles loaded with 1 mM lucigenin at a 5 μM final protein concentration, in the presence of 20 mM KCl. The decrease of lucigenin fluorescence due to Cl^- influx into the vesicles was monitored over time for 25 min. Control experiments were performed by diluting the vesicles in the same way in buffer A without Ure2p, to take into account spontaneous ion leakage. Each point in the diagrams is the difference between the normalized percentages of ion influx obtained in treated and untreated vesicles, respectively. The values shown in each graph were obtained from one experiment out of at least three independent measurements yielding qualitatively identical results.

with PS vesicles (data not shown), in agreement with previous data indicating that these fibrils are not able to interact with the plasma membrane of cultured cells (22).

Ure2p assembly in the presence of phospholipid unilamellar vesicles

A large body of data indicates that lipid membranes can act not only as either surfaces recruiting protein monomers/oligomers and targets of aggregate toxicity, but also as active catalysts of protein aggregation (reviewed in (45)). Having assessed the features of synthetic lipid vesicle permeabilization by Ure2p aggregates and imaged the oligomer/fibril-vesicle interaction, we sought to elucidate whether vesicles with different lipid composition could favor or modify Ure2p aggregation into native-like fibrils. To this purpose, we studied the effect of PC and PS membranes on Ure2p assembly kinetics as monitored by the ThT binding assay (Fig. 5 *A*).

As it has been shown for several proteins, negatively charged PS vesicles enhanced the rate of Ure2p aggregation, whereas no effect was found for neutral PC vesicles. In the presence of PS vesicles, macroscopic aggregates appeared almost immediately after starting the incubation. Still at the earliest measured times, such aggregates increased significantly ThT fluorescence whose maximum value was significantly higher than that measured in the case of Ure2p assemblies formed either in free solution or in the presence of PC vesicles (Fig. 5 *A*). These data suggest that the Ure2p oligomers formed in the early stages of fibril assembly interact preferentially with negatively charged (PS), rather than with neutral (PC), vesicles, possibly through electrostatic interactions between local positively charged amino acid residues or clusters and negatively charged PS headgroups. These data are also consistent with the higher and more-specific permeabilizing effect of Ure2p toxic assemblies on PS vesicles (see above).

The accelerating effect of PS vesicles on Ure2p aggregation led us to consider the possibility that the presence of these vesicles could favor the growth of Ure2p aggregates structurally different from those arising in the absence of phospholipids. We therefore determined whether the interaction between Ure2p and negatively charged PS membranes affected the secondary structure or the oligomeric state of the protein. To investigate whether Ure2p underwent conformational changes upon interaction with PS membranes, we compared the CD spectra of Ure2p in the absence or presence of PC or PS vesicles. No significant spectral changes could be observed immediately after dilution of Ure2p in the lipid suspension (Fig. 5 *B*) and after its incubation with vesicles for up to 48 h (data not shown). Actually, the CD spectra acquired at differing coincubation times (up to 48 h) were superimposable (data not shown) suggesting that the interaction with, and assembly on, PS membranes does not result in significant changes in the secondary structure content of Ure2p by comparision to the spectra recorded for Ure2p alone or in the presence of PC vesicles. This does not exclude differences in the quaternary structure of Ure2p assemblies in the presence or in the absence of PS vesicles.

The morphological features of Ure2p assemblies obtained in the absence or presence of PS vesicles were also studied by electron microscopy (EM) (Fig. 4, *C–F*). Soluble ring-shaped oligomers and native-like fibrils were observed upon

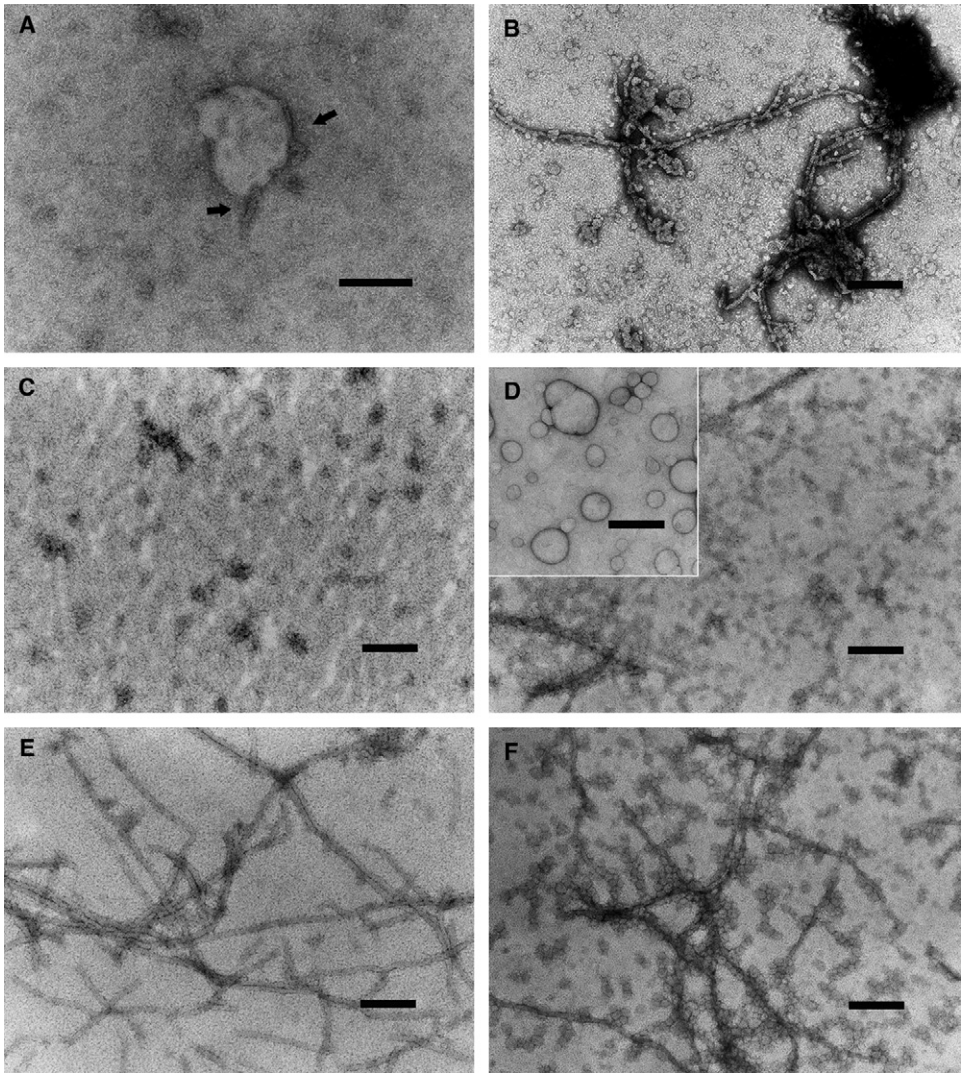

FIGURE 4 EM imaging of the Ure2p-PS vesicle interaction. (*A* and *B*) Negatively stained electron micrographs of PS vesicles treated for 15 min with 10 μM soluble Ure2p oligomers (*A*) or native-like fibrils (*B*). (*C–F*) Negatively stained electron micrographs of Ure2p assembled in the absence (*C* and *E*) or in the presence (*D* and *F*) of PS unilamellar vesicles. (*C* and *D*) Protein oligomers obtained by incubating 50 μM Ure2p for 1 h in the absence (*C*) or in the presence (*D*) of PS. (*E* and *F*) Protein fibrils obtained by incubating 50 μM Ure2p for 48 h in the absence (*E*) or in the presence (*F*) of PS. The inset in panel *D* shows an electron micrograph of control PS vesicles incubated in buffer A for 48 h in the absence of Ure2p. The bars represent 0.2 μm.

incubation of 50 μM Ure2p at 4°C in buffer A for 1 h and 48 h, respectively (Fig. 4, *C* and *E*). These assemblies seemingly correspond to the toxic, native-like species that interact with and permeabilize lipid membranes impairing cell viability (22). EM analysis revealed that Ure2p oligomerizes (Fig. 4 *D*) and assembles into fibrils (Fig. 4 *F*) also in the presence of PS vesicles. Some short fibrils arose as early as 1 h after Ure2p addition to the PS vesicle suspension (Fig. 4 *D*) in agreement with the accelerating effect of PS vesicles on Ure2p polymerization shown by ThT fluorescence (Fig. 5 *A*).

Interestingly, Ure2p fibrillization in the presence of PS vesicles induced vesicle fission into numerous spherical microvesicles that, in turn, coalesced and attached to the surface of the Ure2p assemblies (Fig. 4, *D* and *F*). Such microvesicles were much smaller in size than the PS vesicles incubated for 48 h in the absence of Ure2p (Fig. 4 *F*, *inset*). Vesicle fission, which could be observed also in vesicles treated for 15 min with preformed native-like Ure2p fibrils (Fig. 4 *B*), supports a surface-active behavior of the Ure2p aggregates possibly indicating their amphipathic nature.

The cytotoxic effect of Ure2p oligomers and fibrils obtained in the presence of PS vesicles (imaged in Fig. 4, *D* and *F*, respectively) was tested on H-END cells and compared to the effect of Ure2p native-like assemblies grown in the absence of the vesicles (imaged in Fig. 4, *C* and *E*), previously shown to be highly toxic to this cell type (22). Interestingly, the cytotoxicity to H-END cells of Ure2p oligomers and fibrils formed after 1 h or 48 h of incubation in the presence of PS vesicles was significantly lower relative to that resulting from similar amounts of Ure2p assemblies obtained after identical incubation times in the absence of PS vesicles (Fig. 5 *C*), suggesting that some difference could exist between assemblies formed in the absence or the presence of PS vesicles.

DISCUSSION

A large body of data suggests that surfaces can favor misfolding/unfolding and amyloid aggregation of proteins and peptides. The interaction of protein aggregates with the cell

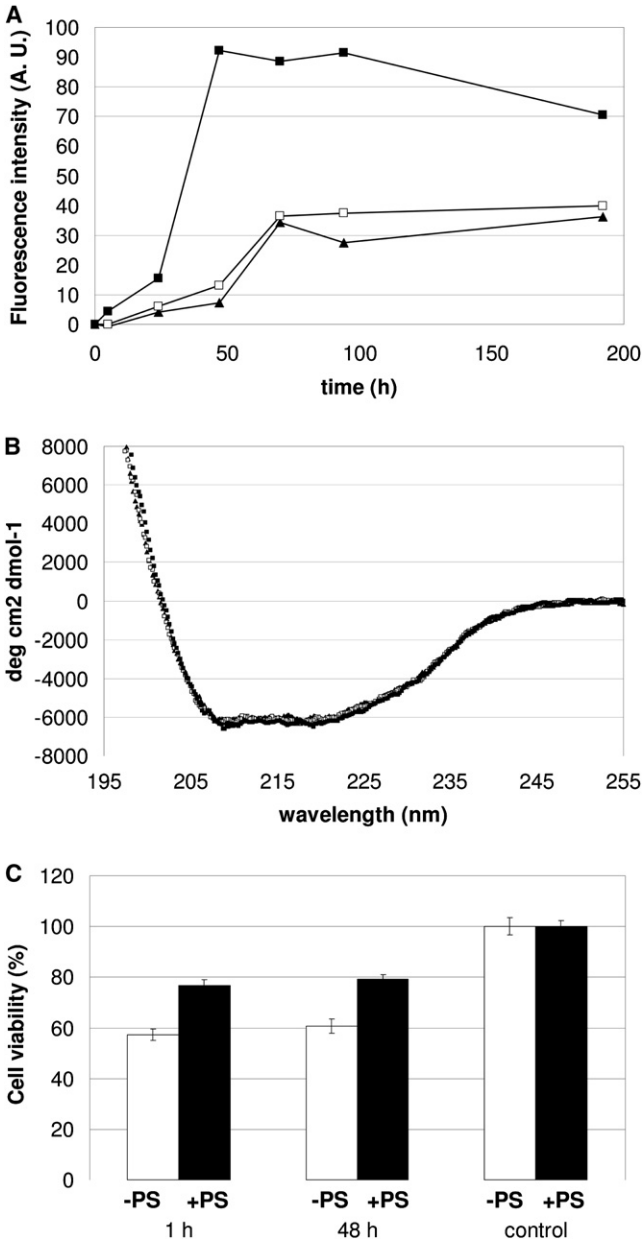

FIGURE 5 PS vesicles affect Ure2p assembly and cytotoxicity. (*A*) Effect of lipid vesicles on the assembly kinetics of Ure2p, monitored by ThT binding assay. Ure2p (50 μM) was assembled at 4°C in buffer A in the absence of lipid vesicles (▲) or presence of PS (■) or PC (□) unilamellar vesicles (1.2 mM). (*B*) Far-UV CD spectra of Ure2p (50 μM) in buffer A in the absence of lipid vesicles (▲) or presence of PS (■) or PC (□) unilamellar vesicles (1.2 mM). The spectra were acquired immediately after thawing Ure2p. (*C*) Viability of H-END cells exposed for 24 h to Ure2p assemblies obtained after 1 h or 48 h of incubation at 50 μM in the absence (*open bars*) or in the presence (*solid bars*) of 0.6 mM PS vesicles. Ure2p oligomers and fibrils were diluted in the culture medium (10 μM final concentration of monomer Ure2p). Cell viability was measured by the MTT assay and expressed as percentage relative to control cells treated with identical volumes of buffer A with or without PS vesicles.

membrane is favored by the presence, in the former, of suitable (i.e., most often hydrophobic) surfaces and, in the latter, of a proper lipid composition (40,41,46). Protein misfolding/unfolding; aggregate nucleation; and recruitment at surfaces, notably lipid membranes, can also be favored by electrostatic interactions (47–50). Actually, it has been repeatedly reported that anionic phospholipids, such as PS, vesicles are putative docking sites for amyloid aggregates or sites where amyloid aggregates can be nucleated thus initiating local membrane disassembly (50–52). Membrane cholesterol, a well-known modifier of membrane fluidity, can also affect the incorporation of toxic aggregates into exposed cells (42,44,53) as well as membrane-associated Abeta peptide fibrillogenesis and Abeta aggregate toxicity in neuronal cells (54). Much less information is available on the interaction between membranes and native-like polymers such as those formed by serpins or by the prion protein Ure2. A first glimpse on this topic has come recently when we have shown that Ure2p native-like oligomers and fibrils can interact with cultured cells modifying membrane permeability and impairing cell viability in a way that is similar to that repeatedly reported for amyloid assemblies in their prefibrillar (or in some cases fibrillar) states (22).

In this study, we have investigated the aggregation features of Ure2p in the presence of synthetic lipid vesicles with different lipid composition, as well as vesicle permeabilization by Ure2p native-like aggregates. We found that the native-like Ure2p assemblies (soluble oligomers and fibrils), previously shown to be cytotoxic by impairing free Ca^{2+} balance in cultured cells (22), are also able to permeabilize synthetic unilamellar, negatively charged, PS and PG vesicles, inducing a significant Ca^{2+} influx and calcein release. No significant permeabilization was induced by the heat-treated amyloid fibrils previously shown to be noncytotoxic (22). This result supports the idea, coming from our previous observations, of a relation between toxicity of native-like Ure2p aggregates and their interaction with the cell membrane. A minor and less-specific effect was observed on zwitterionic PC vesicles treated with the different Ure2p assemblies: PC vesicles were slightly and nonspecifically permeabilized by toxic and nontoxic aggregates. The nonspecific PC vesicle permeabilization by Ure2p heat-treated, amyloid fibrils was abolished when the same vesicles contained moderate amounts of PS. Our data confirm the importance of PS as preferential docking site for toxic Ure2p native-like aggregates and extend similar findings on anionic phospholipid vesicle permeabilization by toxic aggregates of most amyloids (40,41,44).

The ability of Ure2p assemblies to interact with negatively charged phospholipids could appear surprising considering that, under our experimental conditions (pH 7.5), Ure2p has a net negative charge. However, it should be considered that a crucial interaction of the negative lipid surface with clusters of positively charged amino acid residues could occur even in the presence of a net negative charge of the protein. In addition, the strong electrostatic potential on the vesicle membranes could, by itself, favor minute general, or extensive local, conformational rearrangements enhancing

the ability of the Ure2p assemblies to insert within the membrane itself.

Interestingly, PS membrane permeabilization by native-like Ure2p assemblies was abolished by the presence, in the membranes, of cholesterol, whose protective role against aggregate toxicity has been repeatedly described (42,44,53). We did not elucidate the molecular mechanism underlying cholesterol protection against membrane permeabilization; it can be proposed that cholesterol could either hinder the binding of Ure2p toxic aggregates to the membrane or, more generally, increase membrane rigidity and stability, thus reducing aggregate insertion into the bilayer and its subsequent disassembly.

Our findings indicate that vesicle permeabilization to small ions induced by Ure2p oligomers and native-like fibrils is charge dependent, allowing influxes of positively charged ions such as Ca^{2+}, but not of anions such as Cl^{-}. This finding suggests that the passages formed by the Ure2p native-like aggregates into the lipid membranes are electronegative; it also makes unlikely the presence of a significant nonspecific permeabilization arising merely from the presence of discontinuities after membrane disassembly by the aggregates. Soluble Ure2p oligomers and native-like fibrils are built from monomeric units with a net negative charge. We could therefore hypothesize that stretches of the amino-acid sequences of Ure2p oligomers and fibrils insert into the plasma membrane in a way that excludes their negative charges from approaching those of the membrane phospholipids. Such distribution would lead the aggregates to reorganize creating passages in the phospholipid bilayer where the positively charged regions are distributed on the surface of the monomeric units, and the negative regions are located inside the membrane or in the lumen of ring-shaped oligomers. Such organization could favor a preferential influx of positive ions allowing the oligomer to behave as a sort of cation-specific ionophore.

The stronger membrane permeabilization to Ca^{2+} induced by native-like Ure2p fibrils as compared to the soluble oligomers (Fig. 3) agrees with the higher toxicity of fibrils previously observed on H-END cells (22) and could be explained similarly: any damage to the vesicle membrane by native-like fibrils can be more serious because of their larger size and extended surface with increased vesicle interaction and permeabilization. Alternatively, there could also be subtle structural differences in oligomeric and fibrillar Ure2p allowing the latter to better interact with, and permeabilize, synthetic vesicles and cell membranes.

A different mechanism could explain the leakage of calcein, a polyanionic molecule. Calcein (Mr 622.5) is larger than Ca^{2+} (Mr 40.08) or Cl^{-} (Mr 35.45) ions. It could therefore be hypothesized that two possible mechanisms may account for membrane permeabilization by Ure2p native-like, and, in part amyloid, aggregates: besides organizing in passages that are crossed by small ions of opposite charges, the latter could also affect more severely membrane architecture and stability, creating defects in the lipid bilayer and allowing calcein leakage. The appearance of the defects, not seen with small anions such as Cl^{-}, could be favored by the hydrophobic interactions between the four aromatic rings of calcein and the hydrophobic phospholipid tails of the bilayer and could be hindered when the vesicles are rigidified by cholesterol (Fig. 2 *E*).

We showed in this study that PS, but not PC, membranes significantly enhanced Ure2p aggregation into native-like assemblies, in agreement with a number of previously reported data on amyloid aggregation of different peptides and proteins (reviewed in (45)). Our findings extend the view that membranes enriched in anionic phospholipids are enhancers of protein aggregation into amyloid aggregates. We found that Ure2p assembled in the presence of PS vesicles forms oligomers and fibrils morphologically similar to those arising in free solution. This result, together with the close similarity of the CD spectra of Ure2p recorded in the absence or in the presence of PS vesicles, suggests that only minor changes in secondary structure, if any, occur within Ure2p upon its interaction with PS membranes (Fig. 5 *B*). This is further confirmed by the finding that Ure2p aggregates grown in either condition interact similarly with negatively charged membranes, as shown by the EM imaging (Fig. 4).

Interestingly, PS vesicles incubated in the presence of assembling Ure2p underwent massive budding/fission into much smaller spherical microvesicles. Lipid vesicle fission has been widely described as a phenomenon induced either by temperature (55) or by amphiphilic molecules (56,57), although the mechanism of such a process is not clear and its significance controversial. We show here for the first time that synthetic lipid vesicles undergo fission upon interaction with Ure2p native-like aggregates. This finding confirms that the Ure2p oligomeric species formed de novo in the presence of membranes and the preformed native-like Ure2p assemblies (oligomers and fibrils) can intimately and dynamically associate with synthetic lipid vesicles, particularly with the negatively charged ones. Such an association modifies Ure2p assembly, as shown by the increased ThT fluorescence of the assemblies grown in the presence of PS membranes (Fig. 5). More importantly, the interaction with Ure2p also affects the physical stability of the membrane, leading to modifications of the vesicle shape and to vesicle fission. The latter might occur without intensive mixing between the inner and outer compartments of the vesicles, as shown by the selectivity of the vesicle permeabilization, similar to what occurs in cellular processes involving membrane vesiculation.

Finally, Ure2p oligomers and fibrils assembled in the presence of PS vesicles exhibited a significantly reduced cytotoxicity when compared to the native-like oligomers and fibrils formed in the absence of vesicles (Fig. 5 *C*). The reduced cytotoxicity may be due to oligomer and fibril ''coating'' by the lipid microvesicles observed in Fig. 4. Alternatively, the

reduced toxicity may be the consequence of the partitioning of Ure2p assemblies between artificial and cellular membranes, i.e., a lower concentration of Ure2p assemblies available to interact with cell membranes. Ure2p assembly binding to PS microvesicles may result in a partially reduced exposure of the hydrophobic patches responsible of aggregates interaction with, and permeabilization of, cell membranes. However, it cannot be excluded that the lower toxicity stems from a growth path different from that generating toxic native-like oligomers in the absence of phospholipids, with both types of oligomers subsequently evolving into stable, harmless fibrils displaying minute structural differences.

In conclusion, our findings on synthetic lipid vesicles suggest that the previously reported cytotoxicity of native-like Ure2p assemblies could result from their intimate association with the cell membrane leading to lipid bilayer destabilization and formation of ion-selective membrane passages. Differences were seen in Ure2p aggregates grown in the absence or presence of PS lipid bilayers. Both exhibited similar overall structural and morphological features, but the latter grew more rapidly and were less cytotoxic, possibly suggesting minute structural differences. Overall, these data extend to nonamyloid, native-like yeast prion polymers, and possibly to other native-lìke oligomeric and polymeric protein assemblies, the widely recognized effects of amyloid oligomers on lipid membranes and, conversely, of lipid membranes on amyloid oligomer assembly .

SUPPORTING MATERIAL

Two figures are available at http://www.biophysj.org/biophysj/supplemental/S0006-3495(09)00498-6.

This study was supported by grants from the Ente Cassa di Risparmio di Firenze, the Italian MIUR (project PRIN n. 2007XY59ZJ_001), the CNRS, and the ANR (contract No. ANR-06-BLAN-0266).

REFERENCES

1. Prusiner, S. B. 1997. Prion diseases and the BSE crisis. *Science*. 278:245–251.
2. Lacroute, F. 1971. Non-mendelian mutation allowing ureidosuccinic acid uptake in yeast. *J. Bacteriol*. 106:519–522.
3. Magasanik, B. 1992. Regulation of nitrogen utilization. *In* The Molecular and Cellular Biology of the Yeast Saccharomyces cerevisiae., *Vol. 2* E. W. Jones, J. R. Pringle, and J. R. Broach, editors. Cold Spring Harbor Laboratory Press, Plainview, NY, pp. 283–317.
4. Wickner, R. B. 1994. [URE3] as an altered URE2 protein: evidence for a prion analog in Saccharomyces cerevisiae. *Science*. 264:566–569.
5. Edskes, H. K., V. T. Gray, and R. B. Wickner. 1999. The [URE3] prion is an aggregated form of Ure2p that can be cured by overexpression of Ure2p fragments. *Proc. Natl. Acad. Sci. USA*. 96:1498–1503.
6. Masison, D. C., and R. B. Wickner. 1995. Prion-inducing domain of yeast Ure2p and protease resistance of Ure2p in prion-containing cells. *Science*. 270:93–95.
7. Thual, C., A. A. Komar, L. Bousset, E. Fernandez-Bellot, C. Cullin, et al. 1999. Structural characterization of. *Saccharomyces cerevisiae prion-like protein Ure2*. *J. Biol. Chem*. 274:13666–13674.
8. Thual, C., L. Bousset, A. A. Komar, S. Walter, J. Buchner, et al. 2001. Stability, folding, dimerization and assembly properties of the yeast prion Ure2p. *Biochemistry*. 40:1764–1773.
9. Bousset, L., V. Redeker, P. Decottignies, S. Dubois, P. Le Marechal, et al. 2004. Structural characterization of the fibrillar form of the yeast Saccharomyces cerevisiae prion Ure2p. *Biochemistry*. 43:5022–5032.
10. Bousset, L., H. Belrhali, J. Janin, R. Melki, and S. Morera. 2001. Structure of the globular region of the prion protein Ure2 from the yeast. *Saccharomyces cerevisiae*. *Structure*. 9:39–46.
11. Umland, T. C., K. L. Taylor, S. Rhee, R. B. Wickner, and D. R. Davies. 2001. The crystal structure of the nitrogen regulation fragment of the yeast prion protein Ure2p. *Proc. Natl. Acad. Sci. USA*. 98:1459–1464.
12. Coschigano, P. W., and B. Magasanik. 1991. The URE2 gene product of Saccharomyces cerevisiae plays an important role in the cellular response to the nitrogen source and has homology to glutathione s-transferases. *Mol. Cell. Biol.* 11:822–832.
13. Board, P. G., M. Coggan, G. Chelvanayagam, S. Easteal, L. S. Jermiin, et al. 2000. Identification, characterization, and crystal structure of the Ω class glutathione transferases. *J. Biol. Chem.* 275:24798–24806.
14. Bousset, L., H. Belrhali, R. Melki, and S. Morera. 2001. Crystal structures of the yeast prion Ure2p functional region in complex with glutathione and related compounds. *Biochemistry.* 40:13564–13573.
15. Bai, M., J. M. Zhou, and S. Perrett. 2004. The yeast prion protein Ure2 shows glutathione peroxidase activity in both native and fibrillar forms. *J. Biol. Chem.* 279:50025–50030.
16. Taylor, K. L., N. Cheng, R. W. Williams, A. C. Steven, and R. B. Wickner. 1999. Prion domain initiation of amyloid formation in vitro from native Ure2p. *Science.* 283:1339–1343.
17. Sunde, M., L. C. Serpell, M. Bartlam, P. E. Fraser, M. B. Pepys, et al. 1997. Common core structure of amyloid fibrils by synchrotron X-ray diffraction. *J. Mol. Biol.* 273:729–739.
18. Bousset, L., N. H. Thomson, S. E. Radford, and R. Melki. 2002. The yeast prion Ure2p retains its native alpha-helical conformation upon assembly into protein fibrils in vitro. *EMBO J*. 21:2903–2911.
19. Lomas, D. A., and R. W. Carrel. 2002. Serpinopathies and the conformational dementias. *Nat. Rev. Genet*. 10:759–768.
20. Fay, N., V. Redeker, J. Savistchenko, S. Dubois, L. Bousset, et al. 2005. Structure of the prion Ure2p in protein fibrils assembled in vitro. *J. Biol. Chem.* 280:37149–37158.
21. Bousset, L., F. Briki, J. Doucet, and R. Melki. 2003. The native-like conformation of Ure2p in fibrils assembled under physiologically relevant conditions switches to an amyloid-like conformation upon heat-treatment of the fibrils. *J. Struct. Biol.* 141:132–142.
22. Pieri, L., M. Bucciantini, D. Nosi, L. Formigli, J. Savistchenko, et al. 2006. The yeast prion Ure2p native-like assemblies are toxic to mammalian cells regardless of their aggregation state. *J. Biol. Chem.* 281:15337–15344.
23. Rousseau, F., H. Wilkinson, J. Villanueva, L. Serrano, J. W. H. Schymkowitz, et al. 2006. Domain swapping in p13suc1 results in formation of native-like, cytotoxic aggregates. *J. Mol. Biol*. 363:496–505.
24. Stefani, M., and C. M. Dobson. 2003. Protein aggregation and aggregate toxicity: new insights into protein folding, misfolding diseases and biological evolution. *J. Mol. Med.* 81:678–699.
25. Jang, H., B. Ma, R. Lal, and R. Nussinov. 2008. Models of toxic beta-sheet channels of protegrin-1 suggest a common subunit organization motif shared with toxic alzheimer beta-amyloid ion channels. *Biophys. J*. 95:4631–4642.
26. Kourie, J. I. 2001. Mechanisms of prion-induced modifications in membrane transport properties: implications for signal transduction and neurotoxicity. *Chem. Biol. Interact.* 138:1–26.
27. Lin, M. C., T. Mirzabekov, and B. L. Kagan. 1997. Channel formation by a neurotoxic prion protein fragment. *J. Biol. Chem.* 272:44–47.
28. Zhu, M., P. O. Souillac, C. Ionescu-Zanetti, S. A. Carter, and A. L. Fink. 2002. Surface-catalyzed amyloid fibril formation. *J. Biol. Chem.* 277:50914–50922.

29. Sethuraman, A., and G. Belfort. 2005. Protein structural perturbation and aggregation on homogeneous surfaces. *Biophys. J.* 88:1322–1333.

30. Lin, H., R. Bhatia, and R. Lal. 2001. Amyloid beta protein forms ion channels: implications for Alzheimer's disease pathophysiology. *FASEB J.* 15:2433–2444.

31. Relini, A., S. De Stefano, S. Torrassa, O. Cavalleri, R. Rolandi, et al. 2008. Heparin strongly enhances the formation of beta2-microglobulin amyloid fibrils in the presence of type I collagen. *J. Biol. Chem.* 283:4912–4920.

32. Suk, J. Y., F. Zhang, W. E. Balch, R. J. Linhart, and J. W. Kelly. 2006. Heparin accelerates gelsolin amyloidogenesis. *Biochemistry.* 45:2234–2242.

33. Grynkiewicz, G., M. Poenie, and R. Y. Tsien. 1985. A new generation of Ca^{2+} indicators with greatly improved fluorescence properties. *J. Biol. Chem.* 260:3440–3450.

34. Simakova, O., and N. Arispe. 2006. Early and late cytotoxic effects of external application of the Alzheimer's Abeta result from the initial formation and function of Abeta ion channels. *Biochemistry.* 45:5907–5915.

35. McNally, B. A., A. V. Koulov, B. D. Smith, J. B. Joos, and A. P. Davis. 2004. A fluorescent assay for chloride transport; identification of a synthetic anionophore with improved activity. *Chem. Commun.* 2005:1087–1089.

36. Verkman, A. S. 1990. Development and biological applications of chloride-sensitive fluorescent indicators. *Am. J. Physiol. Cell Physiol.* 259:C375–C388.

37. Levine, III, H. 1993. Thioflavine T interaction with synthetic Alzheimer's disease beta-amyloid peptides: detection of amyloid aggregation in solution. *Protein Sci.* 2:404–410.

38. McParland, V. J., N. M. Kad, A. P. Kalverda, A. Brown, P. Kirwin-Jones, et al. 2000. Partially unfolded states of beta(2)-microglobulin and amyloid formation in vitro. *Biochemistry.* 39:8735–8746.

39. Abe, K., and H. Kimura. 1996. Amyloid beta toxicity consists of a Ca(2+)-independent early phase and a Ca(2+)-dependent late phase. *J. Neurochem.* 67:2074–2078.

40. Kourie, J. I., and C. L. Henry. 2002. Ion channel formation and membrane-linked pathologies of misfolded hydrophobic proteins: the role of dangerous unchaperoned molecules. *Clin. Exp. Pharmacol. Physiol.* 29:741–753.

41. Alarcón, J. M., J. A. Brito, T. Hermosilla, I. Atwater, D. Mears, et al. 2006. Ion channel formation by Alzheimer's disease amyloid beta-peptide (Abeta40) in unilamellar liposomes is determined by anionic phospholipids. *Peptides.* 27:95–104.

42. Arispe, N., and M. Doh. 2002. Plasma membrane cholesterol controls the cytotoxicity of Alzheimer's disease AbetaP (1–40) and (1–42) peptides. *FASEB J.* 16:1526–1536.

43. Mirzabekov, T. A., M. C. Lin, and B. Kagan. 1996. Pore formation by the cytotoxic islet amyloid peptide amylin. *J. Biol. Chem.* 271:1988–1992.

44. Lin, M. C., and B. L. Kagan. 2002. Electrophysiologic properties of channels induced by Abeta25–35 in planar lipid bilayers. *Peptides.* 23:1215–1228.

45. Jayasinghe, S. A., and R. Langen. 2007. Membrane interaction of islet amyloid polypeptide. *Biochim. Biophys. Acta.* 1768:2002–2009.

46. Kurganov, B., M. Doh, and N. Arispe. 2004. Aggregation of liposomes induced by the toxic peptides Alzheimer's Abetas, human amylin and prion (106–126): facilitation by membrane-bound GM1 ganglioside. *Peptides.* 25:217–232.

47. Necula, M., C. N. Chirita, and J. Kuret. 2003. Rapid anionic micelle-mediated alpha-synuclein fibrillization in vitro. *J. Biol. Chem.* 278:46674–46680.

48. Kazlauskaite, J., N. Senghera, I. Sylvester, C. Vénien-Bryan, and T. J. Pinheiro. 2003. Structural changes of the prion protein in lipid membranes leading to aggregation and fibrillization. *Biochemistry.* 42:3295–3304.

49. Jayakumar, R., J. Murali, D. Koteeswari, and K. Gomathi. 2004. Cytotoxic and membrane perturbation effects of a novel amyloid forming model peptide poly(leucine-glutamic acid). *J. Biochem.* 136:457–462.

50. Zhao, H., E. K. J. Tuominen, and P. K. J. Kinnunen. 2004. Formation of amyloid fibers triggered by phosphatidylserine-containing membranes. *Biochemistry.* 43:10302–10307.

51. Zhao, H., A. Jutila, T. Nurminen, S. A. Wickström, J. Keski-Oja, et al. 2005. Binding of endostatin to phosphatidylserine-containing membranes and formation of amyloid-like fibers. *Biochemistry.* 44:2857–2863.

52. Lee, G., H. B. Pollard, and N. Arispe. 2002. Annexin 5 and apolipoprotein E2 protect against Alzheimer's amyloid-β-peptide cytotoxicity by competitive inhibition at a common phosphatidylserine interaction site. *Peptides.* 23:1249–1263.

53. Cecchi, C., S. Baglioni, C. Fiorillo, A. Pensalfini, G. Liguri, et al. 2005. Insights into the molecular basis of the differing susceptibility of varying cell types to the toxicity of amyloid aggregates. *J. Cell Sci.* 118:3459–3470.

54. Yip, C. M., E. A. Elton, A. A. Darabie, M. R. Morrison, and J. McLaurin. 2001. Cholesterol, a modulator of a membrane-associated Abeta-fibrillogenesis and neurotoxicity. *J. Mol. Biol.* 311:723–734.

55. Dobereiner, H.-G., J. Kas, D. Noppl, I. Sprenger, and E. Sackmann. 1993. Budding and fission of vesicles. *Biophys. J.* 65:1396–1403.

56. Staneva, G., M. Seigneuret, K. Koumanov, G. Trugnan, and M. I. Angelova. 2005. Detergents induce raft-like domains budding and fission from giant unilamellar heterogeneous vesicles: a direct microscopy observation. *Chem. Phys. Lipids.* 136:55–66.

57. Inaoka, Y., and M. Yamazaki. 2007. Vesicle fission of giant unilamellar vesicles of liquid-ordered-phase membranes induced by amphiphiles with a single long hydrocarbon chain. *Langmuir.* 23:720–728.